Available online at www.sciencedirect.com
ScienceDirect
Advances in Engineering Software 38 (2007) 810–817
ADVANCES IN ENGINEERING SOFTWARE
www.elsevier.com/locate/advengsoft

Numerical modelling of a gravity settler in dynamic conditions

E.F. Gomes [a,*], M.M.L. Guimarães [a], L.M. Ribeiro [b]

[a] Instituto Superior de Engenharia do Porto, Rua Dr. António Benardino de Almeida, 431, 4200-072 Porto, Portugal
[b] Faculdade de Engenharia da Universidade do Porto, Rua Dr. Roberto Frias, 4200-465 Porto, Portugal

Received 17 November 2004; accepted 14 August 2006
Available online 17 January 2007

Abstract

An iterative numerical technique has been developed to simulate in detail the dynamics of a shallow-layer gravity settler. Currently acknowledged models apply only to specific equipments at steady-state and laboratory scale [Jeelani SAK, Hartland S. The continuous separation of liquid/liquid dispersions. Chem Eng Sci 1993;48(2):239–54]. To our knowledge, no study has ever addressed the dynamic simulation of a gravity settler. In this paper a direct numerical technique is presented for computing the thickness and drop-size composition of the dispersion band formed in a shallow-layer settler under steady-state and transient conditions. This technique is an extension for the settler of the one used on the stirred vessel by Ribeiro [Ribeiro LM. Simulação Dinâmica de Sistemas Líquido–Líquido, Um novo Algoritmo com Potencialidades de Aplicação em Controlo. PhD thesis, Universidade do Minho, Portugal; 1995].

Keywords: Numerical simulation; Gravity settler system; Liquid–liquid dispersions

1. Introduction

The importance of separation of immiscible liquid–liquid systems is well known in many industrial fields, such as wastewater treatment and the crude oil industry [7]. Equipments like mixer–settler batteries are commonly used for liquid–liquid extraction and mass transfer processes. Due to the high complexity and cost of the direct experimentation using such equipments, computer simulation becomes very attractive. Algorithms for fast and reliable simulation of single stirred vessels and extraction columns have already been published by some of the present authors, both for steady-state and dynamic conditions [12,11,3–5,14,15].

In general, knowledge about the settler behaviour is scarcer than knowledge about mixers and extraction columns behaviour, both in steady and transient states. Existing models for the settler apply only to specific physical equipments at laboratory scale [6]. More recently, an approach based on the population balance equation has been presented [8,17].

In this paper we describe an algorithm able to simulate transient states in a stirred vessel and gravity settler system (Fig. 1). This approach has been developed from a technique used in the study of the wedge formed in a settler under steady-state conditions [8]. The mathematical model used in this study was proposed by Ruiz for the steady-state operation of a settler with a wedge-shaped dispersion band [16].

2. The mathematical model

To describe the dispersion band transient behaviour of the settler, we adopted a drop population balance equation proposed by Ruiz [16] for the dispersion band at steady-state (Eq. (1)). It describes the drop-number density of drops, $f(v,x)$, with volume v at length co-ordinate x of the settler, as a function of the number of drops entering the elemental volume of the dispersion band per unit time, $F(x)$, the axial velocity of drops in the dispersion band, $U(x)$, and the drop–drop and drop–interface coalescence

* Corresponding author. Tel.: +351 229374488; fax: +351 228321159.
E-mail address: elsag@fe.up.pt (E.F. Gomes).

0965-9978/$ - see front matter
doi:10.1016/j.advengsoft.2006.08.033

Nomenclature

$A(x)$	average projected area of drops at the active interface (L^2)
$C(x,t)$	volume of dispersion coalescing with the active interface (L^3)
$D(x,t)$	volume of dispersion draining with the passive interface (L^3)
$f(v,x)$	drop-number density (L^{-3})
$F(x)$	number of drops entering the elemental volume (L^{-3})
$F(x,t)$	velocity of the inlet dispersion ($L\ T^{-1}$)
$H(x)$	thickness of the dispersion band (L)
h	thickness of the dispersion band (algorithm notation) (L)
hc_t	thickness of the dispersion band (algorithm notation) (L)
h_t	thickness of the dispersion band (algorithm notation) (L)
k	constant defined by Eq. (5) (T^{-1})
M	matrix data structure (algorithm notation)
T	time (T)
$U(x)$	axial velocity of the drops in the dispersion band ($L\ T^{-1}$)
$V(x,t)$	volume of the dispersion band at position x (L^3)
v, v'	drop volume (L^3)
w	settler width (L)
X	length co-ordinate of the settler (L)

Greek letters

α	constant of Eq. (3) ($L\ T^{-1}$)
β	constant of Eq. (6) (L^{-2})
Δt_{long}	time needed for the dispersion to reach each segment (algorithm notation) (T)
δv	incremental volume (L^3)
Δx	small increment in the dispersion band (L)
$\eta(x)$	volume fraction of dispersed phase (hold-up) (dimensionless)
$\eta^*(x)$	surface fraction of dispersed phase (dimensionless)
η_M	maximum volume-packing efficiency (dimensionless)
λ_0	constant of Eq. (2)
$\lambda(v,v')$	drop–drop coalescence frequency (T^{-1})
λ^*	drop–interface coalescence frequency (T^{-1})

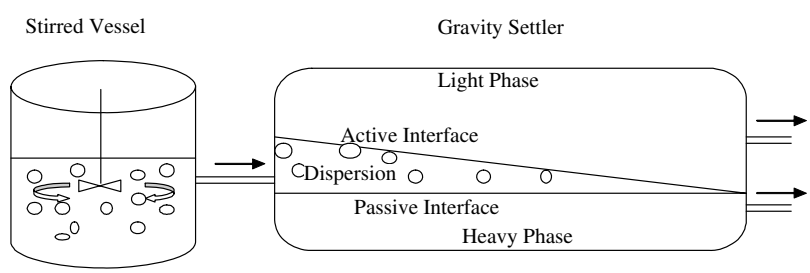

Fig. 1. Stirred vessel and gravity settler system. The dispersion flows into the settler from the vessel, forming a wedge or dispersion band. The drops in the dispersion either coalesce with each other or with the active interface.

frequencies, $\lambda(v,v')$ and $\lambda^*(v)$, respectively. The auxiliary variables $\eta^*(x)$ and $A(x)$ represent, in that order, the surface hold-up and the average projected area of drops at the active interface

$$\frac{\partial}{\partial x}[f(v,x)] = -\frac{w\eta^*(x)\lambda^*(v)}{A(x)}\frac{f(v,x)}{F(x)} - \frac{1}{U(x)F(x)}\left[\int_0^\infty \lambda(v,v')f(v,x)f(v',x)\mathrm{d}v'\right] + \frac{1}{2U(x)F(x)}\left[\int_0^v \lambda(v-v')f(v-v')f(v',x)\mathrm{d}v'\right]. \quad (1)$$

The drop–drop coalescence and the drop–interface frequencies are not amenable to direct determination and are inferred by experimental data [10]

$$\lambda(v,v') = \lambda_0\left(v^{-1/3} + v'^{-1/3}\right)^2, \quad (2)$$

where λ_0 is a parameter which depends upon the physicochemical properties of the system.

This equation contains information about an implicit drop transport mechanism which is vital for building the transient state model. Our algorithm uses this information iteratively to perform integration over time and over space (settler length).

Ruiz employed Gauss–Legendre quadrature for numerically solving the volume integrals and the fourth-order Adams–Moulton predictor–corrector method for the differential equation. In our approach, the discretized form of the population balance equation is solved by a first-order finite difference method with careful control of variable, infinitesimal-like, time and space integration steps.

This computationally simpler approach works quite well, and the algorithm's predictions have been found [2] in agreement with experimental results of Ruiz [16] for the thickness of the wedge.

To describe the behaviour of the stirred-vessel, we adopted, as Ribeiro [13], the mathematical model proposed by Coulaloglou and Tavlarides [1].

The mass-transfer phenomenon is deliberately ignored.

3. The algorithm for the transient state

Our algorithm for the simulation of the transient state of the mixer–settler system iteratively uses the steady-state algorithm to integrate over the time variable, which is consistent with a quasi-steady-state (thermodynamic reversibility) approximation. Starting from the steady-state, we may change one of the operating variables of the vessel (hold-up, flow rate or stirring speed) and simulate the changes on the dispersion band of the settler over time (Fig. 4).

The numerical method works in two steps: space and time integration. The integration over space dimension is the same used by the steady-state algorithm. In this case, the behaviour of the dispersion band is described by discretizing the balance equation. For the representation of drop dimension, a logarithmical grid of volumes is adopted. The wedge of the dispersion band is also divided in elemental segments with length δx, width w (the physical width of the settler) and height $H(x)$, the height of the wedge at co-ordinate x. Each one of these three-dimensional segments is treated as a homogeneous cell within which drop coalescence takes place. A constant axial velocity of the drops with an empirical longitudinal variation is assumed in each cell.

Time integration is necessary in the transient algorithm because changes take place along time in the dispersion entering the settler.

The simulation runs as follows: when the vessel reaches the steady-state for given values of certain operating variables (hold-up, flow rate or stirring speed) the initial wedge is calculated by means of the above referred modified Ruiz [16] steady-state algorithm (Fig. 2).

Next, one of the parameters is step-changed to a new value on the vessel, and, for each time step, a new wedge is calculated from the previous one, as follows: at the ith time step, the dispersion flowing from the vessel to the settler will cause a change in the dispersion band up to the position x_i (Fig. 3). The segments with co-ordinate higher than x_i will not be affected, their properties remaining therefore equal to the ones of the previous state. The simulation continues until a new steady-state of the vessel is reached. The control of the time step takes care of the validity of this assumption.

In the next section we describe the data structure used on the implementation of the algorithm. Using this structure we can efficiently calculate the band thickness for each time step.

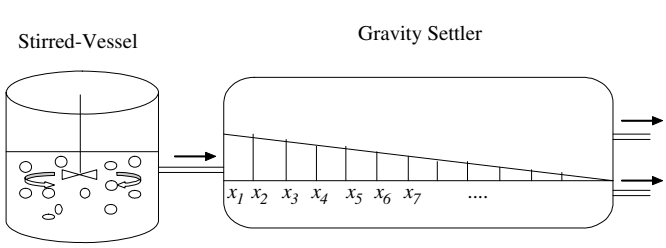

Fig. 2. Dispersion band in steady-state.

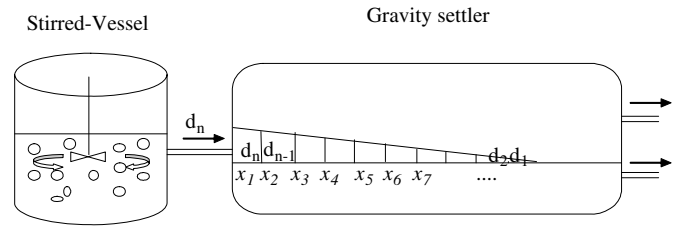

Fig. 3. Dispersion band in transient state for the ith time step.

3.1. Data structure

For each time step t, we calculate the band thickness (or wedge height) $hc_t(x)$, resulting from the composition of the last k wedges for different time steps $h_t(x), h_{t-1}(x), h_{t-2}(x), \ldots, h_{t-k}(x)$, where k depends on the settler length and on

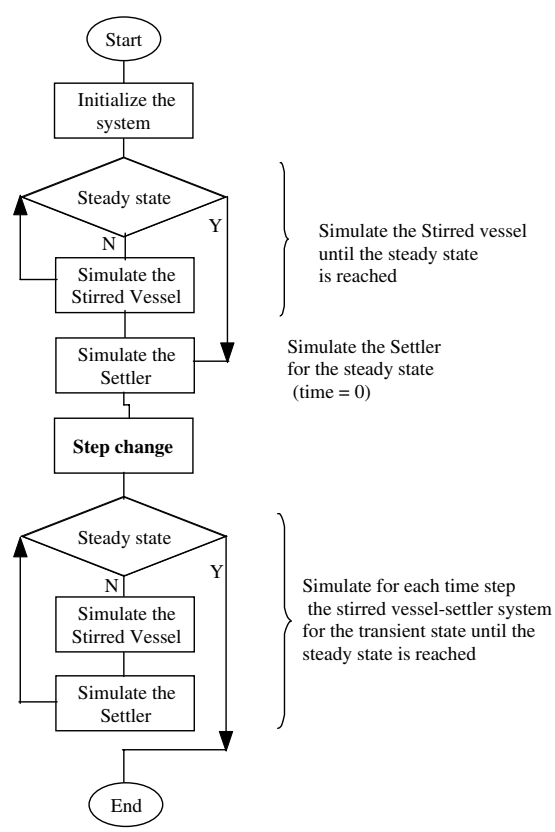

Fig. 4. The algorithm for the simulation of the transient state.

the velocity of the drops, $U(x)$, corresponding to the estimated maximum number of time steps needed to reach the last segment of the wedge.

To implement the method we use a matrix data structure ($M_{i,j}$, $1 \leqslant i \leqslant n\_\text{lin}$, $1 \leqslant j \leqslant n\_\text{col}$) where n_lin is its number of lines, and n_col its number of columns. The value of n_lin is equal to k (see further down). The number of columns, n_col, is equal to the number of points for which we calculate the wedge height. Thus, the value $hc_t(x)$ is stored as $M_{i,j}$, where $i = (t \bmod n\_\text{lin})$ and $j = x$. We are assuming a segment length of 1 cm, which implies $j = x$. Otherwise we would have $j =$ integer part of [x/segment length]. For example, if we are writing the band thickness each 1 cm (segment length) until 100 cm, we have $n\_\text{col} = 100$, $n\_\text{lin} = 100 +$ constant (for example 110) and $hc_{(t \bmod 110)}(x)$. We use this constant because the number of segments reached in each time step depends on $U(x)$ and, when this velocity is in average lower then 1 cm/s, more time then 100 s is needed to reach the last segment of the band thickness. Therefore, we need to use more lines of the matrix. We can calculate n_lin = the integer part of [average $U(x_l)/x_{100} + 1$], $l = 1, 2, \ldots, 100$.

Each sequence of height values corresponding to the wedge height $h(x)$ obtained from the settler routine (Fig. 4) is obliquely written in the matrix starting at line i. For example, in the hypothetical situation where the axial velocity $U(x)$ is constant and equal to 1 cm/s the wedge $h(x)$ would be written on a diagonal. When the writing of the wedge reaches the last line of the matrix M, it continues from the beginning of the matrix reusing the top lines as shown below. At each time step the line i of the matrix have the values of the wedge height for the space discretization used.

3.2. Description of the wedge height calculation

We have described above the data structure that contains the wedge height values. These values are placed on the matrix as follows (we assume once more, for simplicity of explanation, that we have a maximum length of the dispersion band of 100 cm and the value of the space integration step is 1 cm):

- Initially, all the lines of the matrix M are equal and filled with the heights corresponding to the first wedge calculated ($h_1(x)$ corresponding to the initial steady-state).
- For each time step $t > 1$, the new value for position (i,j) of the matrix M is determined as follows:
  - Δt_{long}: this variable represents the time needed for the dispersion to reach each segment. At the beginning of the simulation its value is zero.
  - For each segment $[x-1, x]$ ($x = 1, 2, \ldots, 100$) of the wedge we calculate the value of $h_t(x)$. This value is placed in the i, j position of the matrix.
  - $\Delta t_{\text{long}} = \Delta t_{\text{long}} + 1/U(x)$: the variable is updated according to the axial velocity estimated for the segment;
  - $i =$ the integer part of $[(\Delta t_{\text{long}} + t) \bmod n\_\text{lin}]$;
  - $j = x$.

On the following tables we describe the process using a simplified matrix M with only five lines and five columns, assuming a constant axial velocity equal to 1 cm/s. In each time step Δt_{long} is incremented by 1 unit. We are assuming that the dispersion moves 1 cm/s and each segment is 1 cm long. The first matrix shows M (Fig. 5) after the first time step, when all the lines of the matrix are filled with the values of the steady-state wedge.

In the second time step, the wedge $h_2(x)$ (bold) is written on the diagonal of the matrix M and $hc_2(x)$ (the first line in Fig. 6) is written to the wedge height output file.

In the third time step the wedge $h_3(x)$ is written on the diagonal of the matrix M shown in bold in Fig. 7. When the diagonal reaches the last line of M, the writing continues at the top. Thus, the last value calculated falls on the first line. After that the $hc_3(x)$ (the second line) is written to the output file.

Jumping to the sixth time step, the algorithm writes the wedge $h_6(x)$ (bold) on the diagonal of the matrix M (Fig. 8) and finalizes the step writing $hc_6(x)$ to the output file. In the next time step t the writing restarts on the first line of the matrix M.

1,1	1,2	1,3	1,4	1,5
1,1	1,2	1,3	1,4	1,5
1,1	1,2	1,3	1,4	1,5
1,1	1,2	1,3	1,4	1,5
1,1	1,2	1,3	1,4	1,5

Fig. 5. First matrix M.

2,1	1,2	1,3	1,4	1,5
1,1	**2,2**	1,3	1,4	1,5
1,1	1,2	**2,3**	1,4	1,5
1,1	1,2	1,3	**2,4**	1,5
1,1	1,2	1,3	1,4	**2,5**

Fig. 6. Matrix M at the 2nd time step.

2,1	1,2	1,3	1,4	**3,5**
3,1	2,2	1,3	1,4	1,5
1,1	**3,2**	2,3	1,4	1,5
1,1	1,2	**3,3**	2,4	1,5
1,1	1,2	1,3	**3,4**	2,5

Fig. 7. Matrix M at the 3rd time step.

2,1	**6,2**	1,3	4,4	3,5
3,1	2,2	**6,3**	1,4	4,5
4,1	3,2	2,3	**6,4**	1,5
5,1	4,2	3,3	2,4	**6,5**
6,1	5,2	4,3	3,4	2,5

Fig. 8. Matrix M at the 6th time step.

4. Results

As explained above, the transient algorithm starts from one steady-state and arrives to another steady-state. We have applied the simulation algorithm on data from two sources. First, using experimental data provided by Ruiz [16], second, using data obtained by direct observation of a settler in our laboratory [9].

With respect to the first set of data, the mixer was rectangular, 20 cm long, 20 cm wide and 29 cm high. A Benco Model agitator was used. The impeller was a 10.2 cm diameter curved-blade turbine with six blades and width 1/8 of the diameter. The dispersion left the mixer through a 19 cm wide overflow channel. The settler was a rectangular box of 100 cm long, 20 cm wide and 20 cm high. The settler comprised a narrow chamber, 0.6 cm wide, to receive the entering dispersion. This compartment had a horizontal slot, located 13.5 cm above the base of the settler, with dimensions 19 cm × 0.9 cm, to distribute the dispersion.

The organic phase used consisted of 10% by volume LIX 64N and Chevron ion exchange solvent and the aqueous phase was 0.25 molar sodium sulfate solution (Table 1) [16].

Table 1
Physical properties of the liquid phases (25 °C) – first set of data

	Density (g/cm^3)	Viscosity (cps)	Surface tension (dyne/cm)
0.25 M $NaSO_4$	1.029	1.16	26.8–27.2
10% LIX 64 N Chevron	0.813	1.94	56.4–58.2

Table 2
Physical properties of the liquid phases (25 °C) – second set of data

	Density (g/cm^3)	Viscosity (cps)	Surface tension (dyne/cm)
Na_2SO_4 0.25 M	1.06	0.912	35.6
Kerosene	0.79	1.01	29.4

Regarding the second set of data the mixer was a rectangular box of 10 l capacity and the settler was a rectangular box with 105 cm in length, 20 cm in height and 20 cm in width. The phases were mixed by means of a Rushton impeller, 10 cm diameter, with six flat vertical blades. The flow rates of both phases entering the mixer were directly measured in the pumps after appropriate calibration. The dispersion left the mixer through a 2 × 15 cm slot. A baffle inside the settler allowed the dispersion to enter the settler area with minimum mixer interface.

The aqueous phase was 0.25 molar sodium sulfate solution and the organic phase was kerosene [10], without solute in the system (Table 2).

The parameters λ^* and λ_0 of the mathematical model (Eq. (2)) were adjusted to the experimental data in the two sets of experiments [16,9,10].

In both cases we proceeded as follows. For given pairs of experiments, we compared the results obtained for the band thickness. In the first case we also compared the average volume of the drops (with respect to the second set of data, we have no values to compare). For each pair, one set of conditions corresponds to the start of the dynamic simulation and the other one to the final state.

4.1. First set of data

In Fig. 9 we can see the results obtained for the following pair of conditions: at start, an organic flow rate of 1.2 l/min and a hold-up of 0.5 and at the final state an organic flow rate of 0.88 l/min and a hold-up of 0.37 (a change of −26%). The stirring speed is constant at 360 rpm. The figure shows the evolution of the shape of the dispersion band over time, as calculated by our algorithm, starting from one steady state (the highest curve), and reaching a second steady-state, after 2000 s. The decrease in the organic feed flow rate and, consequently, also in the hold-up causes a significant shortening of the wedge, as expected.

In Fig. 10 we can see a close agreement between the starting and final steady-states results obtained by us and by Ruiz [16]. The comparison of results obtained for other pairs of experiments showed also this good agreement.

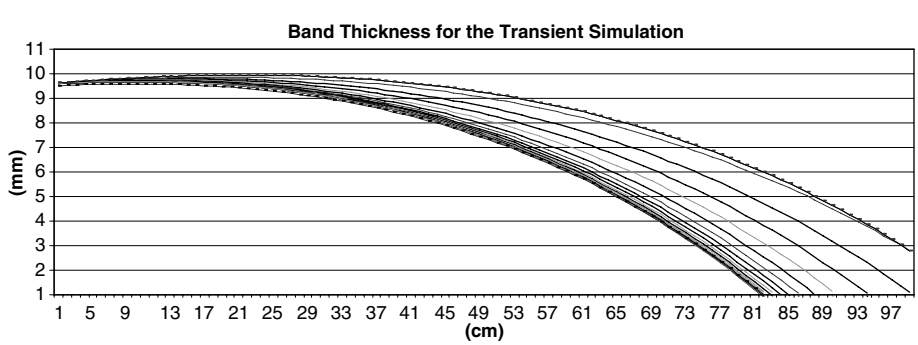

Fig. 9. Each curve represents the simulated band thickness for the transient state at successive points in time (every 100 s), starting from the steady-state (the highest curve) at time zero, and for the following 2000 s.

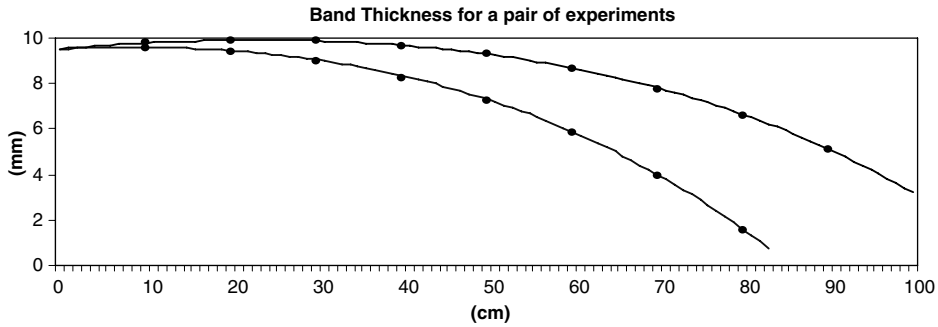

Fig. 10. Each curve represents the simulated band thickness for a steady state obtained by our algorithm. The dots represent the simulated values obtained by Ruiz under the same conditions.

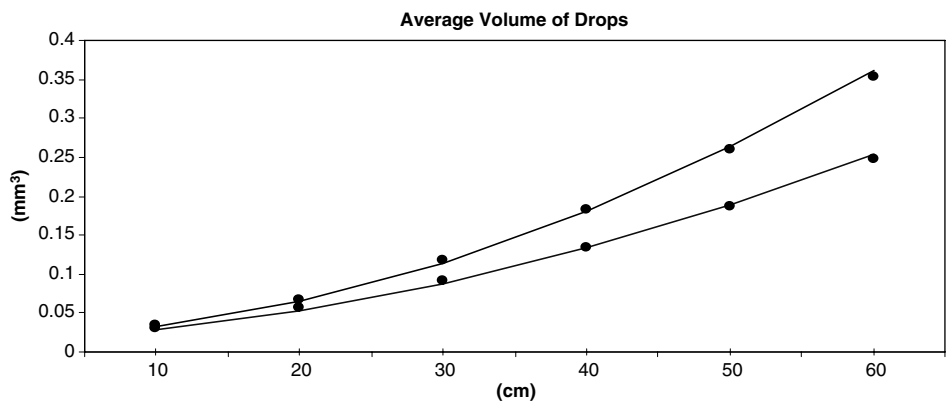

Fig. 11. Each curve represents the simulated average volume of drops for a steady-state obtained by our algorithm. The dots represent the simulated values obtained by Ruiz under the same conditions.

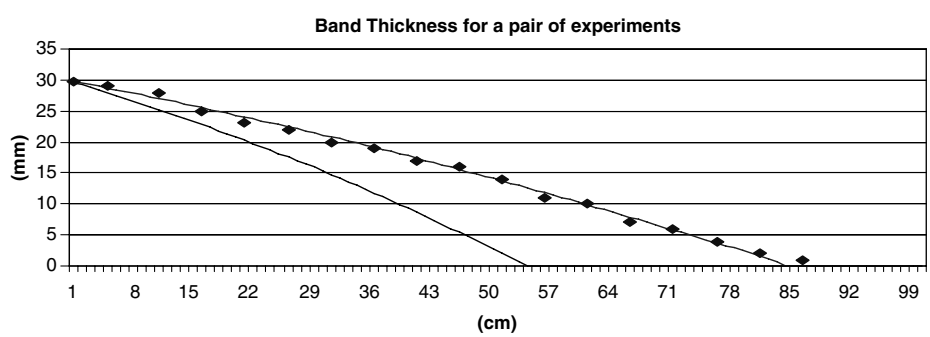

Fig. 12. Each curve represents the simulated band thickness for a steady state obtained by our algorithm. The dots represent the experimental values obtained on our laboratory at the same conditions.

The average volume of drops predicted by the model is presented in Fig. 11. The lowest curve represents the first steady-state and the highest represents the second steady-state. The dots represent the simulated values obtained by Ruiz [16] (we only have information of data up to 60 cm). We observe a close agreement between the starting and final steady-states results obtained by us and by Ruiz for average volume of drops.

4.2. Second set of data

In Fig. 12 we can see the results obtained for the following pair of conditions: at start, a hold-up of 0.3 and an organic flow rate of 1.09 l/min. At the final state, a hold-up of 0.5 and an organic flow rate equal to 2.15 l/min. The stirring speed is constant at 188 rpm.

This figure shows the initial and the final states of the shape of the dispersion band as calculated by our algorithm, starting from one steady state (the lowest curve), and reaching a second steady-state, after 1000 s.

The increase in the hold-up causes a significant enlargement of the wedge, as expected.

5. Conclusions and future work

The results obtained with the developed simulation model for the transient state of the mixer–settler were compared with the values of Ruiz [16] and some experimental

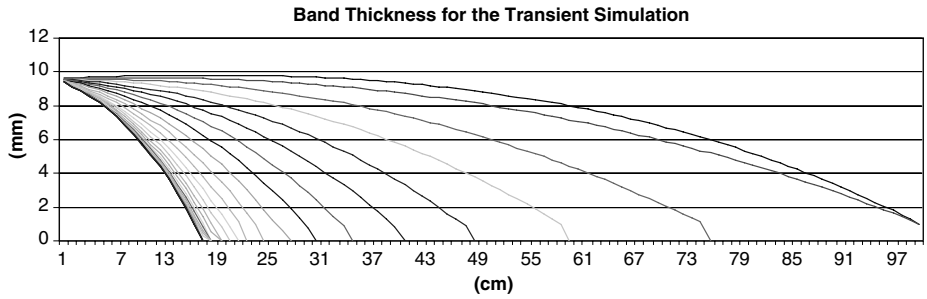

Fig. 13. The simulated band thickness for the transient state at successive points in time (every 100 s), when we decrease the hold-up to a 10th of its initial value.

results obtained in our laboratory [9]. The predicted values for the wedge of the dispersion band compared every 10 cm are in close agreement with the experimental data and those of Ruiz as shown above in the previous section.

The new numerical algorithm here presented has the advantage of adding little complexity for the calculations, being an iterative application of the steady-state algorithm. This algorithm and model seem to be satisfactory for small step-changes. However, for large changes, further validation is needed. It must be noticed that Ruiz's model was developed for a settler that is fed through a slot, the height of which defines the initial thickness of the dispersion band. Fig. 13 shows the results of our algorithm for a large change of the hold-up, reduced from 0.5 to 0.05.

Ruiz's calculation of an initial velocity depending on the initial thickness of the inlet slot of the settler of the dispersion band is also a limitation of her model. To overcome these problems, we are currently working on a new dynamic model using a kinetic formulation in which the movement of the dispersion is modelled as caused by gravity. We propose the following equation for the volume variation over time:

$$\frac{\partial V(x,t)}{\partial t} = F(x,t)w\Delta x + \alpha\left\{\left[\frac{H(x-\Delta x)-H(x)}{\Delta x}\right]-\left[\frac{H(x)-H(x+\Delta x)}{\Delta x}\right]\right\} - \frac{\partial C(x,t)}{\partial t} - \frac{\partial D(x,t)}{\partial t}, \quad (3)$$

where w is the settler width, α is a parameter, $F(x,t)$ is the velocity of dispersion fed into the settler at point x and time t, and H is the thickness of the dispersion band.

The rate of volume loss of the dispersion by coalescence of drops with the active interface, $\partial C(x,t)/\partial t$ is [16]:

$$\frac{\partial C(x,t)}{\partial t} = \frac{w\eta^*(x)\lambda^*(v)}{A(x)}\frac{f(v,x)}{F(x)}\Delta x \cdot v. \quad (4)$$

The rate of volume loss of the dispersion by drainage with the passive interface, $\partial D(x,t)/\partial t$, is

$$\frac{\partial D(x,t)}{\partial t} = kV(x)[(1-\eta(x)) - (1-\eta_{\mathrm{M}})], \quad (5)$$

where k is a constant, V the volume of the dispersion, $\eta(x)$ the hold-up and η_{M} the volume-packing efficiency.

The thickness variation over time is thus given by

$$\frac{\partial H(x,t)}{\partial t} = F(x,t) + \alpha\beta\frac{\partial^2 H(x,t)}{\partial x^2} - \frac{\partial C(x,t)}{\partial t} - \frac{\partial D(x,t)}{\partial t} \quad (6)$$

with $\beta = 1/(w\Delta x)$.

In this way, provision is made for a distributed feed, which may help to explain in a more natural way the often observed initial increase in wedge thickness. The detailed explanation of this mathematical model will be given elsewhere [2].

References

[1] Coulaloglou CA, Tavlarides LL. Description of interaction processes in agitated liquid–liquid dispersions. Chem Eng Sci 1977;32:1289.
[2] Gomes EF, Simulação de Regimes Permanentes e Transitórios de Misturadores–Decantadores, PhD thesis, Universidade do Porto, Portugal, 2006.
[3] Gomes MLN. Comportamento Hidrodinâmico de Colunas Agitadas Líquido–Líquido, PhD thesis, Universidade do Minho, Portugal, 2000.
[4] Guimarães MML, Cruz-Pinto JJC. Mass transfer and dispersed phase mixing in liquid–liquid systems—I. Comput Chem Eng 1988;12:1075.
[5] Guimarães MML, Cruz-Pinto JJC, Regueiras PFR, Madureira CMN. Mass transfer and dispersed phase mixing in liquid–liquid systems—II. Comput Chem Eng 1990;14:139.
[6] Hartland S, Jeelani SAK. In: Godfrey JC, Slater MG, editors. Gravity settler in liquid–liquid equipment. London: John Wiley & Sons; 1994.
[7] Jeelani SAK, Hartland S. The continuous separation of liquid/liquid dispersions. Chem Eng Sci 1993;48(2):239–54.
[8] Padilla, Ruiz, Trujillo. Separation of liquid–liquid dispersions in a deep-layer gravity settler: Part I. Experimental study of the separation process. Hydrometallurgy 1996;42:267–79.
[9] Pinto GA. Optimização Multi-critério da Extracção Líquido–Líquido em Misturadores–Decantadores, PhD thesis, Fac de Engenharia Univ, Porto, 2004.
[10] Pinto GA, Baptista M, Guedes A, Fíuza A, Guimarães MML, Madureira CMN, et al. Model validation for mixer–settler units. In: 6th World congress of chemical engineering, Melbourne, Australia, Conference CD; 2001.
[11] Regueiras PFR, Ribeiro LM, Guimarães MML, Madureira CMN, Cruz-Pinto JJC. Precise and fast computer simulations of the dynamic mass transfer behaviour of liquid–liquid agitated contactors, value adding through solvent extraction. In: Shallcross DC, Paimin R, Prvcic LM, editors. University of Melbourne, vol. 1, Proceedings of ISEC'96; 1996. p. 1031–36.
[12] Regueiras PFR, Gomes ML, Ribeiro LM, Guimarães MML, Cruz-Pinto JJC. Efficient computer simulation of the dynamics of an

agitated liquid–liquid extraction column. In: Proceedings of the 7th international chemical engineering conference, Lisboa, Portugal; 1998.

[13] Ribeiro LM. Simulação Dinâmica de Sistemas Líquido–Líquido, Um novo Algoritmo com Potencialidades de Aplicação em Controlo. PhD thesis, Universidade do Minho, Portugal; 1995.

[14] Ribeiro LM, Regueiras PFR, Guimarães MML, Cruz-Pinto JJC. Numerical simulation of liquid–liquid agitated dispersions on the VAX 6520/VP. Comput Syst Eng 1995;6(4–5):465–9.

[15] Ribeiro LM, Regueiras PFR, Guimarães MML, Cruz-Pinto JJC. The dynamic behaviour of liquid–liquid agitated dispersions. II – Coupled the hydrodynamics and mass transfer. Comput Chem Eng 1996;21(5):543–58.

[16] Ruiz MC. Mathematical modelling of a gravity settler. PhD thesis, University of Utah; 1985.

[17] Ruiz, Padilla. Separation of liquid–liquid dispersions in a deep-layer gravity settler: Part II. Mathematical modelling of the settler. Hydrometallurgy 1996;42:281–91.